

²E. S. Weibel, Phys. Rev. Lett. **2**, 83 (1959).

³N. A. Krall and A. W. Trivelpiece, *Principles of Plasma Physics* (McGraw-Hill, New York, 1973).

⁴R. C. Davidson, D. A. Hammer, I. Haber, and C. E. Wagner, Phys. Fluids **15**, 317 (1972).

⁵R. L. Morse and C. W. Nielson, Phys. Fluids **14**, 830 (1971).

⁶C. E. Max, W. H. Manheimer, and J. J. Thomson, Phys. Fluids **21**, 128 (1978); E. L. Lindman, D. W. Forslund, J. M. Kindel, K. Lee, and W. R. Shanahan, Bull. Am. Phys. Soc. **20**, 1378 (1975); A. Ramani and G. Laval, Phys. Fluids **21**, 980 (1978); R. J. Mason,

"Double Diffusion Hot-Electron Transport in Self-Consistent *E* and *B* Fields" (to be published).

⁷A. B. Langdon and B. F. Lasinski, in *Fusion Research*, edited by J. Killeen, Vol. 16 of *Methods in Computational Physics* (Academic, New York, 1976).

⁸J. J. Thomson, C. E. Max, and K. G. Estabrook, Phys. Rev. Lett. **35**, 663 (1975); B. Bezzerides, D. F. DuBois, D. W. Forslund, and E. L. Lindman, Phys. Rev. Lett. **38**, 405 (1977); W. Woo and J. S. DeGroot, University of California at Davis Report No. UCD PRG R-23, 1977 (to be published).

⁹Kent Estabrook, Phys. Fluids **19**, 1733 (1976).

Fine-Scale Structures in Plasmas Stimulated by a CO₂ Laser

B. Grek, F. Martin, T. W. Johnston, H. Pépin, G. Mitchel, and F. Rheault
Institut National de la Recherche Scientifique, Varennes, Québec J0L2P0, Canada
 (Received 9 August 1978)

Remarkable density structures are observed in the plasma generated during the rise of a high-power CO₂ laser. Jetlike structures and density bowls are seen in interferograms. Infrared imaging shows that these bowls are linked to localized Brillouin-instability backscatter. Depolarization measurements also exhibit filamentary structures that extend far into the underdense regions of the plasma.

Recent publications have demonstrated the importance of radiation-pressure effects in laser-plasma interactions. Interferometric results with subsequent Abel inversion have shown density cavities¹ while small-scale transverse ripples^{2,3} and density steepening^{2,4,5} are evident without inversion. These studies confirmed the existence of plasma density changes due to laser effects at or below the critical density. While profile steepening in the direction of energy flow is of particular importance for compression experiments using a long-wavelength laser, because it enhances energy transport to the core, transverse Rayleigh-Taylor instabilities are considered dangerous in implosions. This latter instability is expected to occur at the ablation layer or in regions of the plasma where the density is greater than the critical density. It is therefore of considerable importance to study the overdense regions of the plasmas, particularly during the rise of the laser pulse when compression is occurring and therefore when the system is most likely to be unstable. There already exists some evidence in x-ray photographs of fine-scale instability generated by laser beams free of "hot spots."^{1,6}

In this Letter we present the first interferometric data with sufficient space-time resolution and a sufficiently high ratio of probe-beam frequency to laser frequency to permit us to re-

solve the temporal evolution of the overdense plasma during the rise of the CO₂ laser. In addition to the interesting results obtained in the above-mentioned publications we have observed (a) an extremely complicated plasma during the first 100 ps; (b) the formation of "jets" that originate deep in the plasma core (at densities greater than 16 times the critical density) and are seen to extend out to at least the critical density layers; (c) cross polarization of the diagnostic laser light in the corona which, in contrast with Faraday-rotation measurements done on plasma formed by 1.06- μm lasers,⁷ form along jets that project from the plasma and tend to be stronger near the plasma edges; (d) the formation of low-density "bowls" that are evident in the plasma up to 4 or 5 times the critical density; (e) that these bowls are linked either to Brillouin-driven density compression or to filamentation.⁸

The CO₂ laser used in these experiments consisted of a conventional mode-locked oscillator, optical gate, and two stages of amplification. It produced 10–12 J of 10.6- μm radiation in a 1.2–1.7-ns (full-width at half maximum) pulse. The target was a ribbon of 150- μm -thick polyethylene. After obtaining preliminary interferometric results and observing the unusual structures presented here, we made a considerable effort to characterize the energy distribution at the focus

of our off-axis parabolic mirror used in focusing the laser, in particular to ascertain whether there were any significant hot spots in the laser flux distribution.⁹ The measurements were made by use of a film technique¹⁰ with visible-light afterexposure, and extra SF₆ attenuation¹¹ in the CO₂-laser amplifier isolater. The results are presented in Fig. 1 and show (a) no evident incident laser hot spots and (b) a peak intensity of roughly 10¹⁴ W/cm². Since some of the plasma structures are quite reproducible, one may conclude that unobservably slight local but consistent intensity variations in the focused CO₂-laser beam can produce important plasma profile modification, and that it may require unrealistically smooth beams of suppress this behavior, at least on planar targets.

Interferograms were taken with a 20-ps ruby laser that was synchronized to the CO₂ laser through the use of a common acoustic mode-locking system.¹² The jitter between the two lasers is estimated to be much less than the 200 ps which was our temporal resolution for this measurement. This well-synchronized, short ruby pulse that is considerably shorter than the main CO₂ pulse allowed us to measure the temporal evolution of the plasma up to densities greater than 10 times the critical density on a shot-to-shot basis. The interferometer used was a modified Weinberg-Wood¹³ interferometer whose final adjustment was done with white light. A selection of interferometric results are shown in Figs. 2 and

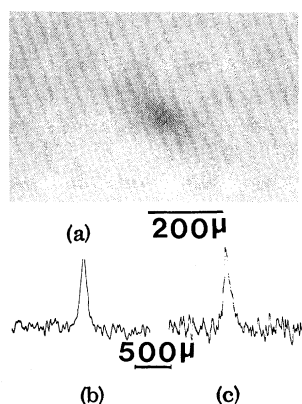


FIG. 1. (a) Photograph of the energy distribution in the focal spot of the $f/1.5$ off-axis parabola. (b), (c) Densitometer traces along the vertical (interferometer line of sight) and horizontal (CO₂-laser polarization direction) axes of (a). The half-energy-point separations are 100 μm by 160 μm along elliptic axes implying a peak flux of about 10¹⁴ W/cm².

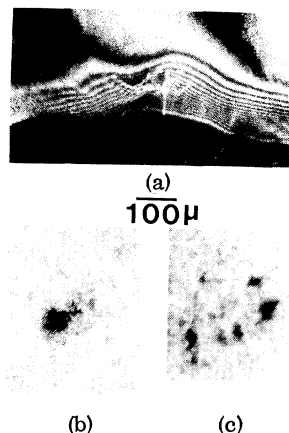


FIG. 2. (a) Interferogram of the plasma taken 700 ps after the beginning of the CO₂-laser pulse. (b) Infrared image of the plasma taken at the same time as (a). (c) Infrared image of the plasma on a subsequent shot, showing multiple infrared-emission spots.

3. In addition the strong refraction of the probing beam tends to generate "false fringes" that occur in a region of strong density gradients.¹⁴ In particular we have observed such fringes in schlieren and shadowgraphy photographs. In interpreting our interferograms it should be kept in mind that one fringe corresponds to a density-length product of $(10^{19} \text{ electron/cm}^3) \times 100 \mu\text{m}$. The critical density occurs therefore after about two fringes. The interferogram in Fig. 2 that was taken 700 ps after the start of the CO₂-laser pulse shows most of the typical structures observed in our experiments. In particular we note the bowl that is formed in the subcritical regions of the plasma a little to the left of center in the

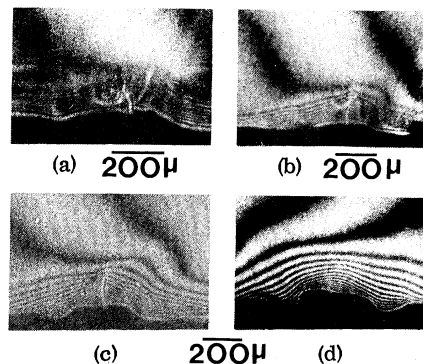


FIG. 3. Interferograms of the plasma taken (a) 100 ps (b) 800 ps, (c) 900 ps, and (d) 1.2 ns after the beginning of different CO₂-laser shots.

picture. Figure 2(b) shows the focal spot imaged using the time-integrated backscattered infrared light.¹⁰ This photograph was taken on the same shot as the interferogram. The position and size of the dark spot in the infrared image correspond to the bowl-shaped depression in the interferogram. These bowls always originate at or below the critical density and end at about 4 to 5 times the critical density. In general we see many more backscatter spots as shown in Fig. 2(c). However in these cases the bowl formation is not as clearly visible in the interferograms. Spectroscopic measurements of the backscattered light show that the backscattered emission is increasingly red-shifted at higher energies, as found in a previous study,¹⁵ and that more hot-spot emission is seen at higher energies. We can therefore link the formation of these bubbles to Brillouin backscatter emission either as primary cause⁸ or in association with filamentation.⁸ Some possible consequences of these bubbles is their tendency to encourage Rayleigh-Taylor instabilities and the generation of strong magnetic fields.¹⁶ Examination of the interferogram in Fig. 2(a), and particularly the ones in Figs. 3(b) and 3(c), shows bright lines that are perpendicular to the fringes. These light lines always originate at the critical density and penetrate the plasma to densities greater than 16 times the critical density.

In regions of the plasma where these "filaments" are observed, the fringes bend outward in the outer regions of the plasma. However in some cases we found that in regions of overdense plasma the fringes bend inward. This indicates that large amounts of plasma are being transported outwards from the overdense regions of the plasma along these filaments. Since this is an instability that (i) originates in overdense plasma, (ii) occurs only during the rise of the CO₂ pulse when the electromagnetic pressure is increasing, and (iii) involves gross transport of plasma, it is tempting to associate it with a type of Rayleigh-Taylor instability, with the increasingly intense electromagnetic field playing the role of the accelerated light fluid. The bright line or filament is tentatively interpreted as being a caustic generated by the plasma jet that carries the heavier plasma out. On the other hand, although computer simulation of large-amplitude filamentation behavior⁸ has not given results at large plasma densities, it may be from lack of trying with our parameters, including an increasing electromagnetic flux.

As shown in Fig. 3(a), at time less than about 100 ps after the start of the CO₂-laser pulse the plasma density is extremely complicated and filled with such jets. Insufficient time-space resolution could well result in the plasma being characterized as "turbulent," as has apparently been done elsewhere.¹⁷

Figure 3(c) shows an interferogram taken 900 ps after the beginning of the CO₂ pulse. There is still one caustic between the remnants of two "bowls" that extend into 4 or 5 times the CO₂ critical density. Figure 3(d) was taken 1.2 ns after the beginning of the CO₂ pulse and shows that after the laser peak, hydrodynamic "healing" smooths out much of the complex structure observed previously. The fringes are now much sharper than previously, indicating a more quiescent plasma.

Figures 4(a) and 4(b) show images of the plasma that were obtained by placing the plasma between two crossed polarizers and illuminating it with a 1-2-ns ruby-laser pulse, the short-pulse system undergoing modification at the time. In Fig. 4(a) the ruby pulse was centered on the rising part of the CO₂-laser pulse, whereas in Fig. 4(b) it was centered slightly after the peak. These photographs also show jetlike cross-polarization structures extending far into the underdense corona of the plasma. This result and the interpretation that the overdense jets seen in our interferograms are the result of a Rayleigh-Taylor instability are consistent with the forms in the simulations of Mima, Tajima, and Leboeuf¹⁶ on magnetic field generation. It should also be

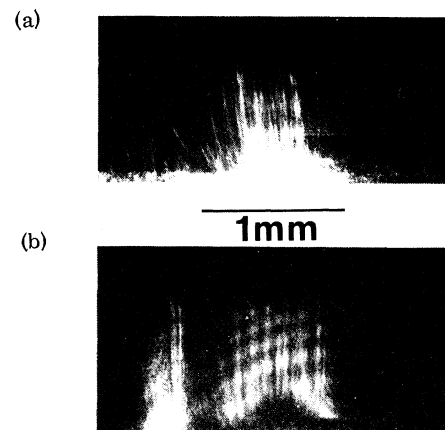


FIG. 4. "Faraday rotation" photographs of the plasma taken with a 2-ns ruby-laser probe pulse: (a) during the CO₂-laser pulse, and (b) just after the peak of the CO₂-laser pulse.

pointed out that a breakup of these "jets" into apparently still finer filaments, as is becoming apparent in Fig. 4(b), becomes even more pronounced at later times. On the other hand, depolarization from plasma density structures without magnetic field is possible,¹⁸ but how these structures could retain their form without any associated magnetic field is difficult to explain.

Although considerable density structure has been expected and observed in the underdense plasma and near critical density, we have presented results that show that the entire plasma displays very complicated density behavior during the rise of the CO₂-laser pulse. In addition we have found that plasma transport from the ablation layer is in our case dominated by instabilities in the overdense plasma that may well generate complex magnetic fields even in the underdense plasma. It therefore appears that stable adiabatic compression of laser targets is more difficult than foreseen, both to understand and to improve. Obviously more work needs to be done before an adequate knowledge of the problems in laser fusion is achieved.

¹T. P. Donaldson and I. J. Spalding, Phys. Rev. Lett. **36**, 467 (1976).

²D. T. Attwood, D. W. Sweeney, J. M. Auerbach, and P. H. Y. Lee, Phys. Rev. Lett. **40**, 184 (1978).

³J. F. Reintjes, T. N. Lee, R. C. Eckardt, and R. A. Andrews, J. Appl. Phys. **47**, 4457 (1976).

⁴R. Fedosejevs, I. V. Tomov, N. H. Burnet, G. D.

Enright, and M. C. Richardson, Phys. Rev. Lett. **39**, 932 (1977).

⁵H. Azechi, S. Oda, K. Tanaka, T. Norimatsu, T. Sasaki, T. Yamanaka, and C. Yamanaka, Phys. Rev. Lett. **39**, 1144 (1977).

⁶R. A. Haas, M. H. Boyle, K. R. Manes, and J. E. Swain, J. Appl. Phys. **47**, 1318 (1976).

⁷J. A. Stamper, E. A. Mclean, and B. H. Ripin, Phys. Rev. Lett. **26**, 1177 (1978).

⁸K. Estabrook, Phys. Fluids **19**, 1733 (1976); W. L. Kruer, E. J. Valeo, and K. G. Estabrook, University of California Radiation Laboratory Report No. UCRL-76612, 1975 (unpublished).

⁹R. P. Haas, H. D. Shay, W. L. Kruer, M. J. Boyle, D. W. Phillion, F. Rainer, V. C. Rupert, and H. N. Kornblum, Phys. Rev. Lett. **39**, 1533 (1977).

¹⁰G. Mitchel, B. Grek, F. Martin, H. Pépin, F. Rheault, and H. Baldis, to be published.

¹¹As SF₆ is a nonlinear absorber, it will tend to accentuate any nonuniformities of the laser beam.

¹²B. Grek, F. Martin, F. Rheault, and H. Pépin, to be published.

¹³F. J. Weinberg and N. B. Wood, J. Sci. Instrum. **36**, 227 (1959).

¹⁴C. M. Vest, Appl. Opt. **14**, 1601 (1975); M. M. Mueller, Los Alamos Scientific Laboratory Report No. LA-VR-77-2469, 1977 (unpublished).

¹⁵B. Grek, H. Pépin, T. W. Johnston, J. N. Leboeuf, and H. A. Baldis, Nucl. Fusion **17**, 1165 (1977).

¹⁶K. Mima, T. Tajima and J. N. Leboeuf, Phys. Rev. **41**, 1715 (1978).

¹⁷Y. V. A. Zakkarenkov, N. N. Zorev, O. N. Krokhin, Y. U. A. Mikhaslov, A. A. Rupajov, G. V. Sklizkov, and A. S. Shikanov, Zh. Eksp. Teor. Fiz. **70**, 547 (1976) [Sov. Phys. JETP **43**, 283 (1976)].

¹⁸R. Lemberg and J. Stamper, Phys. Fluids **21**, 814 (1978).

Retardation of Dislocation Generation and Motion in Thin-Layered Metal Laminates

S. L. Lehoczky

McDonnell Douglas Research Laboratories, McDonnell Douglas Corporation, St. Louis, Missouri 63166

(Received 2 August 1978)

The yield strengths of thin-layered Al-Cu and Al-Ag laminates greatly increase as the layer thicknesses are reduced. This strength enhancement is interpreted as evidence for the retardation of dislocation generation and motion as has been theoretically proposed.

Several years ago, Koehler¹ proposed that a laminate structure which is formed of thin layers of two metals, *A* and *B*, where one metal (*A*) has a high dislocation-line energy and the other metal (*B*) has a low dislocation-line energy, should exhibit a resistance to plastic deformation and brittle fracture well in excess of that for homogeneous alloys. If the dislocation-line energies are so mismatched, the termination of the motion of dislocations in metal *B* is energetically

favored over a dislocation propagation across the layer interface into metal *A*. In the case of thick layers, the dislocations generated in either of the layers will pile up in *B* at the *B-A* interface and thereby provide the stress concentrations needed for premature yield. Hence, to suppress the generation of new dislocations in the layers, the thicknesses of *A* and *B* must be small.

In this Letter we report experimental results for the layer-thickness dependence of the yield

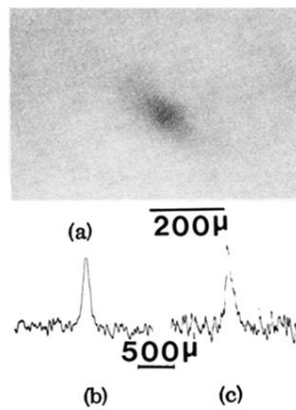


FIG. 1. (a) Photograph of the energy distribution in the focal spot of the $f/1.5$ off-axis parabola. (b), (c) Densitometer traces along the vertical (interferometer line of sight) and horizontal (CO_2 -laser polarization direction) axes of (a). The half-energy-point separations are $100 \mu\text{m}$ by $160 \mu\text{m}$ along elliptic axes implying a peak flux of about 10^{14} W/cm^2 .

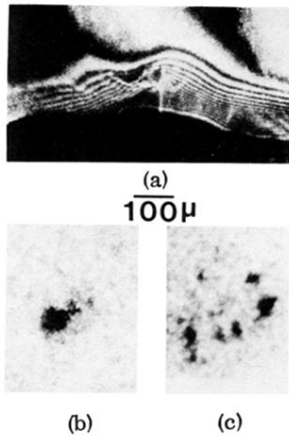


FIG. 2. (a) Interferogram of the plasma taken 700 ps after the beginning of the CO_2 -laser pulse. (b) Infrared image of the plasma taken at the same time as (a). (c) Infrared image of the plasma on a subsequent shot, showing multiple infrared-emission spots.

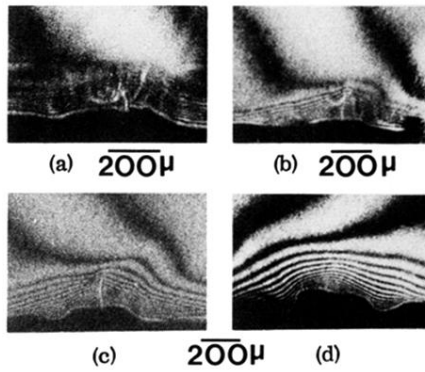


FIG. 3. Interferograms of the plasma taken (a) 100 ps (b) 800 ps, (c) 900 ps, and (d) 1.2 ns after the beginning of different CO_2 -laser shots.

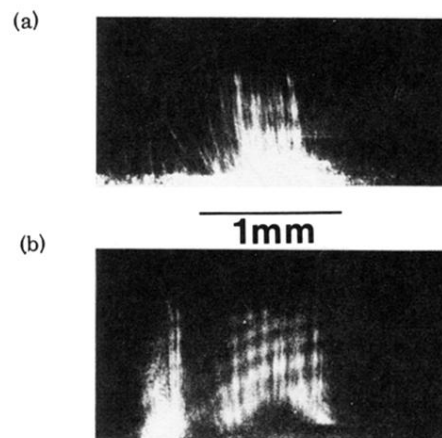


FIG. 4. "Faraday rotation" photographs of the plasma taken with a 2-ns ruby-laser probe pulse: (a) during the CO_2 -laser pulse, and (b) just after the peak of the CO_2 -laser pulse.